ウスやラットの in vivo 実験において、薬物間相互作用を評価するためのプローブ化合物として利用可能である。

F.健康危険情報
なし

G.研究発表
Kuroda M, Kusuhara H, Endou H, Sugiyama Y. Rapid elimination of cefaclor from the cerebrospinal fluid is mediated by a benzylpenicillin-sensitive mechanism distinct from organic anion transporter 3.
J Pharmacol Exp Ther. 314:855-61, 2005

H.知的財産権の出願・登録状況
なし

研究成果の刊行に関する一覧表

書籍

該当なし

雑誌

発表者氏名	論文タイトル名	発表誌名	巻号	ページ	出版年
Kuroda M, Kusuhara H, Endou H, Sugiyama Y.	Rapid elimination of cefaclor from the cerebrospinal fluid is mediated by a benzylpenicillin-sensitive mechanism distinct from organic anion transporter 3.	J Pharmacol Exp Ther.	314	855-861	2005

研究成果の刊行に関する一覧表

書籍

該当なし

雑誌

発表者氏名	論文タイトル名	発表誌名	巻号	ページ	出版年
Inoue, K., Denda, M., Tozaki, H., Fujishita, K., Koizumi, S. and Inoue, K.	Characterization of multiple P2X receptors in cultured normal human epidermal keratinocytes.	J.Invest. Dermatol	124	756-763	2005
Narita, M., Miyatake, M., Shibasaki, M., Tsuda, M., Koizumi, S., Narita, M., Yajima, Y., Inoue, K. and Suzuki, T.	Long-lasting change in brain dynamics induced by methamphetamine: enhancement of protein kinase C-dependent astrocytic response and behabioral sensitization.	J. Neurochem.	93	1383-1392	2005
Nasu-tada, K., Koizumi, S. and Inoue, K.	The involvement of β1 integnin in microglial chemotaxis and proliferation on fibronectin:different regulations by ADP through PKA.	Glia	52	98-107	2005
Fujishita, K., Koizumi, S. and Inoue, K	Upregulation by retinoic acid of P2Y2 receptors in normal human epidermal keratinocytes.	Purinergic Signaling,			IN PRESS
Nasu-Tada, K. *, Koizumi, S.*, Tsuda, M.*, Kunifusa, E. and Inoue, K.	Possible involvement of increase in spinal fibronectin following peripheral nerve injury in upregulation of microglial $P2X_4$, a key molecule for mechanical allodynia.	Glia			IN PRESS
小泉修一、藤下加代子、津田誠、井上和秀	ATP を介した皮膚ケラチノサイト間情報連絡と痛み、	Pain Research			IN PRESS
小泉修一、藤下加代子、津田誠、井上和秀	G 蛋白共役型 ATP 受容体と痛み	Pain Clinic			IN PRESS

Shuto H, Yamauchi A, Ikeda M, Sohda Y, Koga A, Tominaga K, Egawa T, Kataoka Y	Forced exercise-induced flushing of tail skin in ovariectomized mice, as a new experimental model of menopausal hot flushes	J. Pharmacol. Sci.	98	323-326	2005
Yamauchi A, Shuto H, Dohgu S, Nakano Y, Egawa T, Kataoka Y	Cyclosporin A aggravates electroshock-induced convulsions in mice with a transient middle cerebral artery occlusion	Cell. Mol. Neurobiol.,	25	923-928	2005

Kuroda M, Kusuhara H, Endou H, Sugiyama Y.	Rapid elimination of cefaclor from the cerebrospinal fluid is mediated by a benzylpenicillin-sensitive mechanism distinct from organic anion transporter 3.	J Pharmacol Exp Ther.	314	855-861	2005

Characterization of Multiple P2X Receptors in Cultured Normal Human Epidermal Keratinocytes

Kaori Inoue,* Mitsuhiro Denda,* Hidetoshi Tozaki,†‡ Kayoko Fujishita,† Schuichi Koizumi,§ and Kazuhide Inoue†‡

*Shiseido Research Center, Yokohama, Japan; †Division of Biosignaling, National Institute of Health Sciences, Tokyo, Japan; ‡Graduate School of Pharmaceutical Sciences, Kyushu University, Fukuoka, Japan; §Division of Pharmacology, National Institute of Health Sciences, Tokyo, Japan

ATP-gated ion channels (P2X) are expressed in human epidermis and cultured keratinocytes. The aim of this study was to characterize native P2X receptors in normal human epidermal keratinocytes (NHEK) using whole-cell patch clamp technique, RT-PCR, and determination of intracellular Ca^{2+} concentration ($[Ca^{2+}]_i$). Application of ATP resulted in an inward current with a reversal potential of 0 mV. Response to ATP showed two types of currents: the slowly desensitizing response and the rapidly desensitizing response. The slowly desensitizing response was blocked by iso-pyridocaphosphate-6-azophenyl-2′, 5′ disulfonic acid (PPADS), a P2X receptor antagonist. We found that the expression of multiple $P2X_2$, $P2X_3$, $P2X_5$, and $P2X_7$ receptor subtype mRNA was increased in differentiated cells. On the other hand, the expression of G-protein-coupled $P2Y_2$ mRNA was downregulated in differentiated cells. Increases in $[Ca^{2+}]_i$ evoked by αβ-methylene ATP (αβ-meATP) and 2′, 3′-O-(4-benzoylbenzoyl) ATP (BzATP) were elevated, whereas elevation of $[Ca^{2+}]_i$ evoked by uridine 5′-triphosphate (UTP) was decreased in differentiated cells. Application of ATP or UVB radiation increased the expression of $P2X_1$, $P2X_2$, $P2X_3$, and $P2X_7$ receptors in NHEK. Changes in the expression levels and cation influx via multiple P2X receptors might be involved in the regulation of differentiation and one of the epidermal external sensors.

Key words: ATP/channel/differentiation/intracellular calcium
J Invest Dermatol 124:756–763, 2005

ATP is released from a variety of tissues (Milner *et al*, 1990; Hansen *et al*, 1993; Ferguson *et al*, 1997) and acts as one of the mediators to transmit signals to the central and peripheral nervous system (for reviews, see Burnstock and Wood, 1996; Thorne and Housley, 1996; Norenberg and Illes, 2000; North and Surprenant, 2000). ATP receptors (P2 receptors) are classified broadly within two families; ligand-gated ion channels (P2X) and G-protein-coupled metabotropic receptors (P2Y). P2X receptors have seven subtypes ($P2X_{1-7}$) and form heteromeric or homomeric channel assemblies.

Strong evidence has been accumulated, which states that ATP regulates the structure of skin systems by acting as an important messenger via the intermediary of P2 receptors (Pillai and Bikle, 1992; Dixon *et al*, 1999; Greig *et al*, 2003; Koizumi *et al*, 2004). For instance, ATP increases DNA synthesis (Pillai and Bikle, 1992) and cell number in keratinocytes (Greig *et al*, 2003). Keratinocytes constantly release ATP whether skin is damaged or not (Dixon *et al*, 1999; Cook and McCleskey, 2002). Koizumi *et al* (2004) reported that Ca^{2+} waves evoked by mechanical stimulation in cultured normal human epidermal keratinocytes (NHEK) were heavily dependent on release and diffusion of ATP. This extracelluar ATP is a dominant messenger in cell-to-cell communication and in turn activates $P2Y_2$ receptors. As for the expression of P2 receptors in human skin, $P2Y_1$ and $P2Y_2$ receptors are relatively expressed in the basal layer and their localization is associated with the proliferation stage (Dixon *et al*, 1999; Greig *et al*, 2003). The expression of $P2Y_2$ mRNA is downregulated in differentiating HaCaT keratinocytes (Koegel and Alzheimer, 2001; Burrell *et al*, 2003). On the other hand, $P2X_5$ and $P2X_7$ receptors are expressed in the suprabasal layer, spinosum layer, and granular layer and their localization is associated with the differentiation or terminal differentiation phases (Greig *et al*, 2003). Moreover, P2X receptors play a role in delayed barrier recovery in hairless mouse epidermis when topical ATP and αβ-methylene ATP (αβ-meATP) are applied (Denda *et al*, 2002). But, research has still not been carried out with regard to the functional roles of all P2X receptors in cultured NHEK.

The aim of our study is to clarify which P2X receptor subtypes are expressed in NHEK using electrophysiological methods. Furthermore, we also provide evidence that P2X receptor expression is affected by the differentiation phase, application of ATP and UVB radiation *in vitro*, using RT-PCR methods, and monitoring free intracellular calcium concentration ($[Ca^{2+}]_i$).

Abbreviations: αβ-meATP,α,β-methylene ATP; BzATP, 2′, 3′-O-(4-benzoylbenzoyl) ATP; $[Ca^{2+}]i$, intracellular Ca^{2+} concentration; 2MeSADP, 2-methylthioadenosine 5′-diphosphate; NHEK, normal human epidermal keratinocytes; PPADS, iso-pyridocaphosphate-6-azophenyl-2′, 5′, disulfonic acid

Results

Characterization of ATP-activated inward currents ATP evoked inward currents in keratinocytes (67 of 168 cells) loaded with 2 mM GDPβ. Response to ATP showed two

Copyright © 2005 by The Society for Investigative Dermatology, Inc.

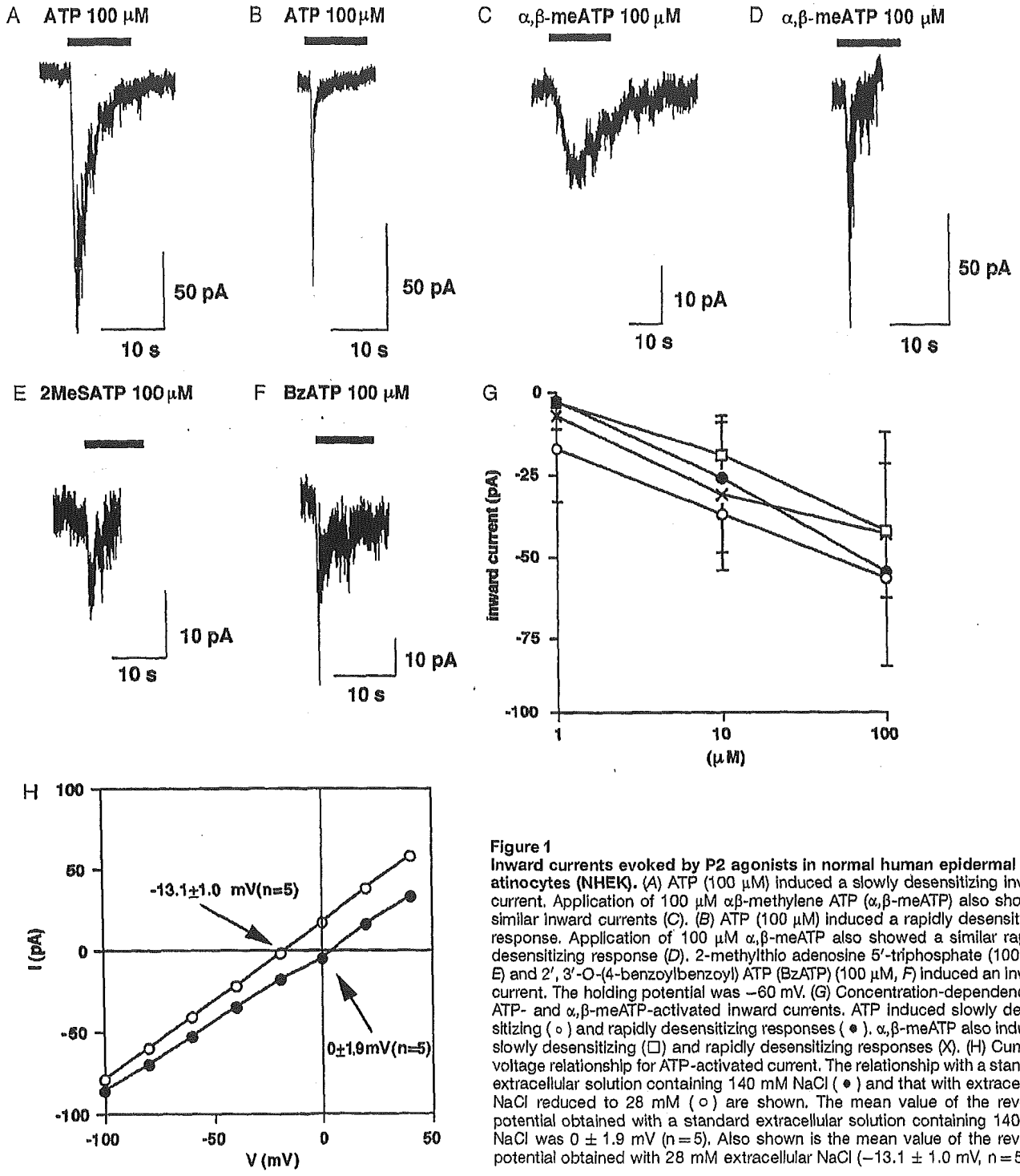

Figure 1
Inward currents evoked by P2 agonists in normal human epidermal keratinocytes (NHEK). (*A*) ATP (100 μM) induced a slowly desensitizing inward current. Application of 100 μM αβ-methylene ATP (α,β-meATP) also showed similar inward currents (*C*). (*B*) ATP (100 μM) induced a rapidly desensitizing response. Application of 100 μM α,β-meATP also showed a similar rapidly desensitizing response (*D*). 2-methylthio adenosine 5′-triphosphate (100 μM, *E*) and 2′, 3′-O-(4-benzoylbenzoyl) ATP (BzATP) (100 μM, *F*) induced an inward current. The holding potential was −60 mV. (*G*) Concentration-dependency of ATP- and α,β-meATP-activated inward currents. ATP induced slowly desensitizing (○) and rapidly desensitizing responses (●). α,β-meATP also induced slowly desensitizing (□) and rapidly desensitizing responses (X). (H) Current–voltage relationship for ATP-activated current. The relationship with a standard extracellular solution containing 140 mM NaCl (●) and that with extracellular NaCl reduced to 28 mM (○) are shown. The mean value of the reversal potential obtained with a standard extracellular solution containing 140 mM NaCl was 0 ± 1.9 mV (n = 5). Also shown is the mean value of the reversal potential obtained with 28 mM extracellular NaCl (−13.1 ± 1.0 mV, n = 5).

types of currents, that is, a slowly desensitizing (Fig 1*A*) and a rapidly desensitizing response (Fig 1*B*). The fraction of ATP-responding cells with a rapidly desensitizing current was 36% (24 of 67). The remaining cells, approximately 64%, showed a slowly desensitizing response. Of 88 cells tested, 14 cells responded to ATP and αβ-meATP (100 μM), 23 cells responded only to ATP, and the remaining 51 cells responded to neither ATP nor αβ-meATP. The values of the peak amplitudes by ATP and αβ-meATP (100 μM), a $P2X_1$, $P2X_3$, and $P2X_{2/3}$ receptors agonist, with rapidly desensitizing responses were −54.7 ± 32.8 pA (n = 11) and −43.3 ± 19.4 pA (n = 6), respectively (Fig 1*B*, *D*, and *G*). The responses to the second application by these agonists were not observed. The peak values of the slowly desensitizing response to ATP and αβ-meATP (100 μM) were −56.8 ± 26.8 pA (n = 10) and −42.3 ± 30.3 pA (n = 13) (Fig 1*A*, *C*, and *G*). ATP and αβ-meATP evoked inward currents concentration-dependently in both types of responses (Fig 1*G*). The slowly desensitizing responses to αβ-meATP (10 μM) were inhibited by iso-pyridocaphosphate-6-

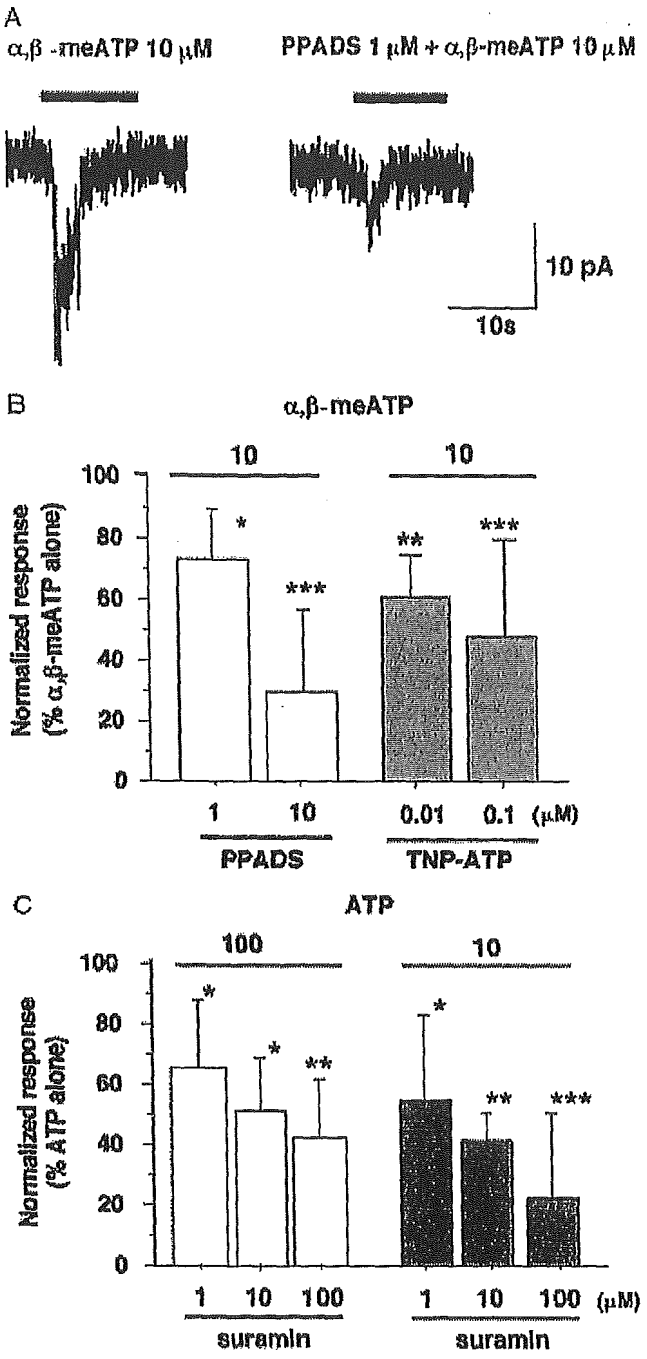

Figure 2
Inhibitory effects because of antagonists in response to ATP and αβ-methylene ATP (α,β-meATP) with slowly desensitizing currents. (*A*) Suppression of ATP-activated current because of P2X antagonist iso-pyridocaphosphate-6-azophenyl-2′, 5′ disulphonic acid (PPADS). (*B*) Concentration-dependency of inhibitory effects of PPADS (1 and 10 μM) and 2′,3′-*O*-(2,4,6-trinitrophenyl) adenosine 5′-triphosphate (10 and 100 nM) on α,β-meATP-activated currents (*$p<0.05$, **$p<0.01$, ***$p<0.001$ compared with the response of 10 μM α,β-meATP alone). Antagonists were applied to the cells 2 min before and during the α,β-meATP application. (*C*) Concentration-dependency of inhibitory effects of suramin on ATP-activated currents (*$p<0.05$, **$p<0.01$, ***$p<0.001$ compared with the response of ATP alone). Suramin was applied to the cells 2 min before and during the ATP application. The holding potential was −60 mV.

azopheny l–2′, 5′ disulfonic acid (PPADS; 1 and 10 μM; 72.3% ± 14.9% and 29.4% ± 25.4%; n = 3–7, Fig 2*A* and *B*) and 2′,3′-*O*-(2,4,6-trinitrophenyl) adenosine 5′-triphosphate (TNP-ATP; 10 and 100 nM; 62.5% ± 12.1% and 47.9% ± 32.0%; n = 4–11, Fig 2*B*), a $P2X_1$, $P2X_{2/3}$, and $P2X_3$ antagonist. This indicates that an inward current was evoked by the activation of $P2X_{2/3}$ receptors. The non-specific P2 receptor antagonist suramin concentration-dependently inhibited the ATP-activated current (Fig 2*C*). ATP-activated current (10 μM; 32.7 ± 20.5 pA, n = 3) in αβ-meATP-insensitive cells was blocked by PPADS (1 μM; 32.7% ± 9.8%, n = 3, $p > 0.001$). This indicates that an inward current was evoked by the activation of $P2X_2$ and $P2X_5$ receptors. The response to 2′, 3′-O-(4-benzoylbenzoyl) ATP (BzATP; 10 μM, −38.1 ± 24.2 pA, n = 6) was equal to ATP (−39.0 ± 17.1 pA, n = 6) and BzATP-activated current was inhibited by brilliant blue G (BBG; 1 μM; 41.5% ± 29.8%; n = 6, $p > 0.001$). BBG blocks rat $P2X_2$ receptors (Jiang *et al*, 2000), human $P2X_5$ receptors (Bo *et al*, 2003), and human $P2X_7$ receptors (Jiang *et al*, 2000). Each IC_{50} value on the ATP-activated current is 1370 nM in rat $P2X_2$ receptors and is 530 nM in human $P2X_5$ receptors. The IC_{50} value on the BzATP-activated current is 265 nM in human $P2X_7$ receptors (Jiang *et al*, 2000). Although ATP and BzATP were equipotent with respect to current responses, these responses seem to be evoked by the activation of $P2X_2$, $P2X_5$, and/or $P2X_7$ receptors in the present study. The slowly desensitizing response to 2-methylthio adenosine 5′-triphosphate (2MeSATP; 100 μM, −22.6 ± 8.4 pA, n = 6) was also smaller than the ATP-evoked current. This response was also insensitive to αβ-meATP and not inhibited by PPADS. This indicates that an inward current was evoked by the activation of $P2X_4$.

Figure 1*H* shows the measurement of the reversal potential of the ATP-activated current. To determine the ionic selectivity of the ATP-activated conductance, the reversal potential was measured in the presence of decreased extracellular NaCl in the cells loaded with 2 mM GDPβ. The reversal potential became more negative when the extracellular NaCl was decreased to 28 mM (Fig 1*H*). A negative shift in the reversal potential with a decreased NaCl concentration indicates that the ATP-activated conductance via P2X receptors is selective to cations. On the other hand, in the case of the ATP-activated conductance via P2Y receptors, the mean value of the reversal potential obtained with a standard extracellular solution was −18.5 ± 3.4 mV (*n* = 5) in the cells loaded with 0.3 mM GTP. A positive shift in reversal potential with a decreased NaCl concentration (−6.0 ± 3.0 mV, n = 5) indicates that the ATP-activated conductance via P2Y receptors conductance is selective to anions.

Comparison of the $[Ca^{2+}]_i$ response by P2 agonists between proliferating and differentiating keratinocytes Next, we investigated whether the differentiation stage in NHEK affects functional P2 receptor expression using a Ca^{2+} imaging method. Increase in $[Ca^{2+}]_i$ by ATP was not influenced by the absence of external Ca^{2+} ($0Ca^{2+}$) in proliferating subconfluent cells (Fig 3*A*). This indicates that the increase of $[Ca^{2+}]_i$ was dependent on the intracellular Ca source, suggesting the involvement of

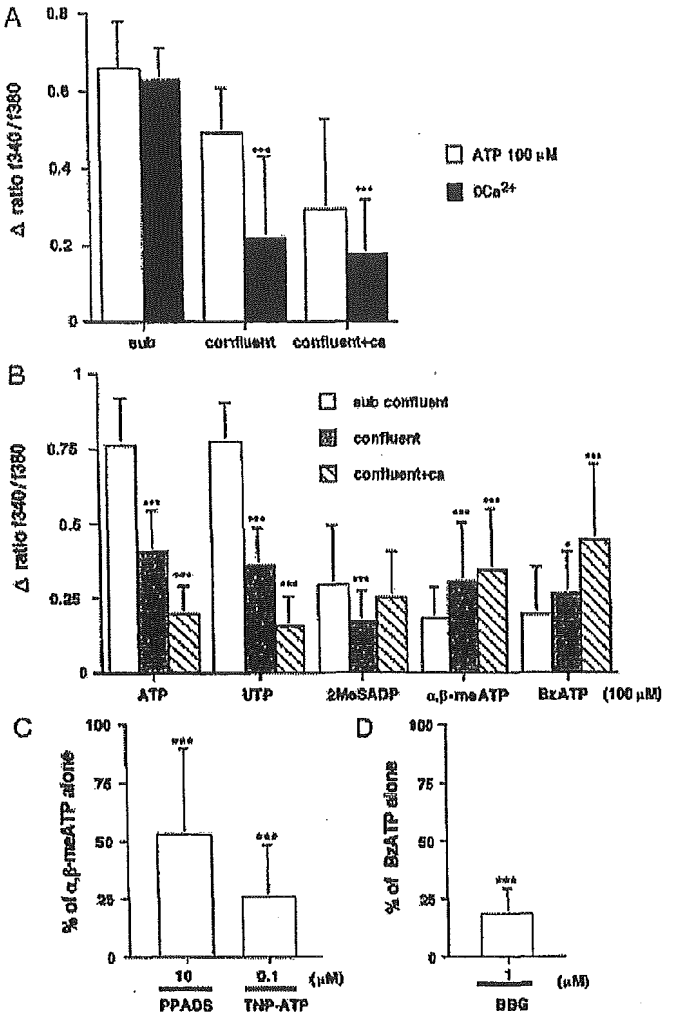

Figure 3
Characterization of P2 receptor-mediated Ca^{2+} responses in proliferated or differentiated keratinocytes. (*A*) Effect of extracellular Ca^{2+} on ATP-evoked increases in $[Ca^{2+}]_i$ in proliferating subconfluent cells (subconfluent) or differentiating over-confluent cells (confluent and confluent + Ca). ATP was applied to normal human epidermal keratinocytes (NHEK) for 20 s. Results were obtained from all cells (n = 62–113), which were tested from two different strains of NHEK. These histograms show a comparison of significant differences from the responses evoked by 100 μM ATP in the absence ($0Ca^{2+}$) or presence of extracellular Ca^{2+} (***$p < 0.001$). (*B*) Pharmacological characterization of Ca^{2+} responses in the different culture conditions. Results were obtained from all cells (n = 109–273), which were tested from two different strains of NHEK. *$p < 0.05$ and ***$p < 0.001$ compared with the response evoked by ATP analogues in subconfluent cells. (*C*) Isopyridocaphosphate-6-azophenyl-2′, 5′ disulphonic acid (10 μM) and 2′,3′-*O*-(2,4,6-trinitrophenyl) adenosine 5′-triphosphate (100 nM) inhibited the α,β-meATP-evoked increases in $[Ca^{2+}]_i$ in differentiating over-confluent cells. Antagonists were applied to the cells 5 min before and during the α,β-meATP application. Results were obtained from 59 to 160 tested (at least two independent experiments using two strain of NHEK). ***$p < 0.001$ compared with the response evoked by 100 μM α,β-meATP alone. (*D*) Brilliant blue G (BBG) (1 μM) inhibited the BzATP-evoked increases in $[Ca^{2+}]_i$ in differentiating over-confluent cells. BBG was applied to the cells 5 min before and during the BzATP application. Results were obtained from 124 to 210 tested (at least two independent experiments using two strain of NHEK). ***$p < 0.001$ compared with the response evoked by 100 μM BzATP alone.

G-protein-coupled P2Y receptors. On the other hand, increase in $[Ca^{2+}]_i$ by ATP was influenced by the absence of external Ca^{2+} in differentiating over-confluent cells (Fig 3*A*). This indicates that the increase of $[Ca^{2+}]_i$ was dependent on the extracellular Ca^{2+}, suggesting the involvement of P2X receptors. The rank order of the Ca^{2+} response was ATP = uridine 5′-triphosphate (UTP) > 2-methylthioadenosine 5′-diphosphate (2MeSADP) > αβ-meATP = BzATP in proliferating subconfluent cells (Fig 3*B*). On the other hand, the rank order of the Ca^{2+} response in differentiating over-confluent cells (confluent + ca) was BzATP > αβ-meATP > 2MeSADP > ATP = UTP (Fig 3*B*). PPADS (10 μM) and TNP-ATP (100 nM) inhibited the αβ-meATP-evoked $[Ca^{2+}]_i$ increase (53.0% ± 36.1%; n = 73, 25.7% ± 22.6%; n = 60, Fig 3*C*). BBG (1 μM) inhibited the BzATP-evoked $[Ca^{2+}]_i$ increase (18.2% ± 10.8%; n = 124, Fig 3*D*). These results suggest that $P2X_1$, $P2X_{2/3}$, or $P2X_3$, and $P2X_7$ receptors were responsible for the responses in differentiating over-confluent cells.

Changes in P2X and P2Y receptor subtypes mRNA expression P2X and P2Y receptors have a different pattern of localization in the skin (Greig *et al*, 2003). We investigated whether their expression was influenced by culture conditions. Figure 4 shows the expression patterns of mRNA for P2 receptors under the different conditions. We detected the expression of $P2X_1$, $P2X_4$, $P2X_5$, $P2X_7$ (weak signal or not), $P2Y_1$, and $P2Y_2$ in subconfluent proliferating cells. The expression of $P2X_2$, $P2X_3$, $P2X_5$, and $P2X_7$ receptor subtypes was upregulated in differentiated cells whereas $P2X_1$ was downregulated at the stage of differentiation. The expression of $P2X_4$ and $P2Y_1$ receptor subtypes was not changed by any culture conditions. On the other hand, the expression of $P2Y_2$ mRNA was downregulated in differentiated cells. $P2X_6$ receptors were not expressed under these culture conditions (data not shown).

A large amount of ATP was released from NHEK because of damage or mechanical stimulation (Cook and McCleskey, 2002; Koizumi *et al*, 2004). It is well known that UVB causes skin inflammation. NHEK will be exposed to ATP in irritated skin. We also investigated whether autocrine stimulation (application of ATP) and a type of external stimulation such as UVB radiation changed P2X and P2Y receptor subtype expression. Application of ATP (300 μM) increased the expression of $P2X_1$, $P2X_2$, $P2X_3$, and $P2X_7$ receptor subtypes. UVB radiation (30 or 60 mJ per cm^2) specifically increased the expression of $P2X_1$, $P2X_3$, and $P2X_7$ receptor subtypes. The expression of $P2X_4$, $P2X_5$, and $P2Y_1$ receptor subtypes was not changed by the application of ATP or UVB radiation. The expression of $P2Y_2$ receptor was downregulated under both conditions. Cytotoxicity was not observed in any case of the conditions for 6 h (legend of Fig 4).

Discussion

This study is an analysis of the electrophysiological properties of P2X receptors in NHEK. We found that the expression of multiple P2X receptor subtypes was influenced during the differentiation phase. NHEK was stimulated by ATP and UVB treatments, which in turn affected P2X receptor expression. We determined that the P2X receptors are present in NHEK and are subject to the following conditions. The reversal potential of ATP-evoked current was

0 mV and the conductance is selective to cations in GDPβs-loaded cells. P2X agonists produced a rapidly desensitizing response in NHEK as well as in DRG neurons (Grubb and Evans, 1999). Furthermore, the ATP-evoked increase of $[Ca^{2+}]_i$ was influenced by the absence of extracellular Ca^{2+} in differentiating over-confluent cells.

P2X receptors were classified within several subtypes, based on their sensitivity to agonists and antagonists, or the time course of their desensitization because of currents (Evans and Surprenant, 1996). $P2X_1$ and $P2X_3$ receptors are characterized by their sensitivity to αβ-meATP and a rapidly desensitizing current. $P2X_2$ and $P2X_{4-7}$ receptors are characterized by insensitivity to αβ-meATP and a slowly desensitizing current. Although homomeric $P2X_2$ receptors are insensitive to αβ-meATP, heteromeric $P2X_{2/3}$ receptors are characterized by their sensitivity to αβ-meATP and a slowly desensitizing current (Lewis *et al*, 1995; Ueno *et al*, 1998). Additionally, the responses of the currents are categorized by their sensitivity to the P2X antagonist PPADS. PPADS antagonized $P2X_1$, $P2X_2$, $P2X_3$, $P2X_{2/3}$, $P2X_5$, and $P2X_7$, but not $P2X_4$ or $P2X_6$. In this study, αβ-meATP-activated currents have the following features: their responses may be rapidly or slowly desensitizing currents; the slowly desensitizing currents were inhibited by PPADS and TNP-ATP. These results suggest that $P2X_1$, $P2X_{2/3}$, and $P2X_3$ receptors were responsible for the responses. ATP-activated currents that yield slowly desensitizing responses have the following features: these responses were insensitive to αβ-meATP, and inhibited by PPADS. ATP-activated current with a slowly desensitizing response however was not inhibited by PPADS in some of cells. Furthermore, the current responses attained because of BzATP and 2MeSATP support our characterization of $P2X_2$, $P2X_4$, $P2X_5$, and/or $P2X_7$. Although it is evident from the results of current responses and RT-PCR that $P2X_1$, $P2X_{2/3}$, $P2X_3$, $P2X_4$, and $P2X_5$ receptors are functional in proliferating subconfluent cells, their contribution seems minimal as the ATP-evoked increases of $[Ca^{2+}]_i$ were not influenced by the absence of extracellular Ca^{2+} in proliferating subconfluent cells (Fig 3). Furthermore, UTP and ATP evoked the same increases of $[Ca^{2+}]_i$ in the presence of extracellular Ca^{2+}. These results coincide with previous researches that indicated that it is the $P2Y_2$ receptors that play a functional role in the proliferated phase (Dixon *et al*, 1999; Lee *et al*, 2001; Burrell *et al*, 2003; Greig *et al*, 2003). Although UTP activates $P2Y_2$ and $P2Y_4$ receptors, the $P2Y_4$ subtype is a functional receptor in HaCaT keratinocytes but not in NHEK (Burrell *et al*, 2003).

$P2Y_2$ receptors respond to ATP in the proliferated phase; however, in the differentiated phase, it is the P2X receptors that mediate a greater response from ATP (Fig 3). Only differentiated over confluent cells were affected by the absence of extracellular Ca^{2+}. There were higher increases

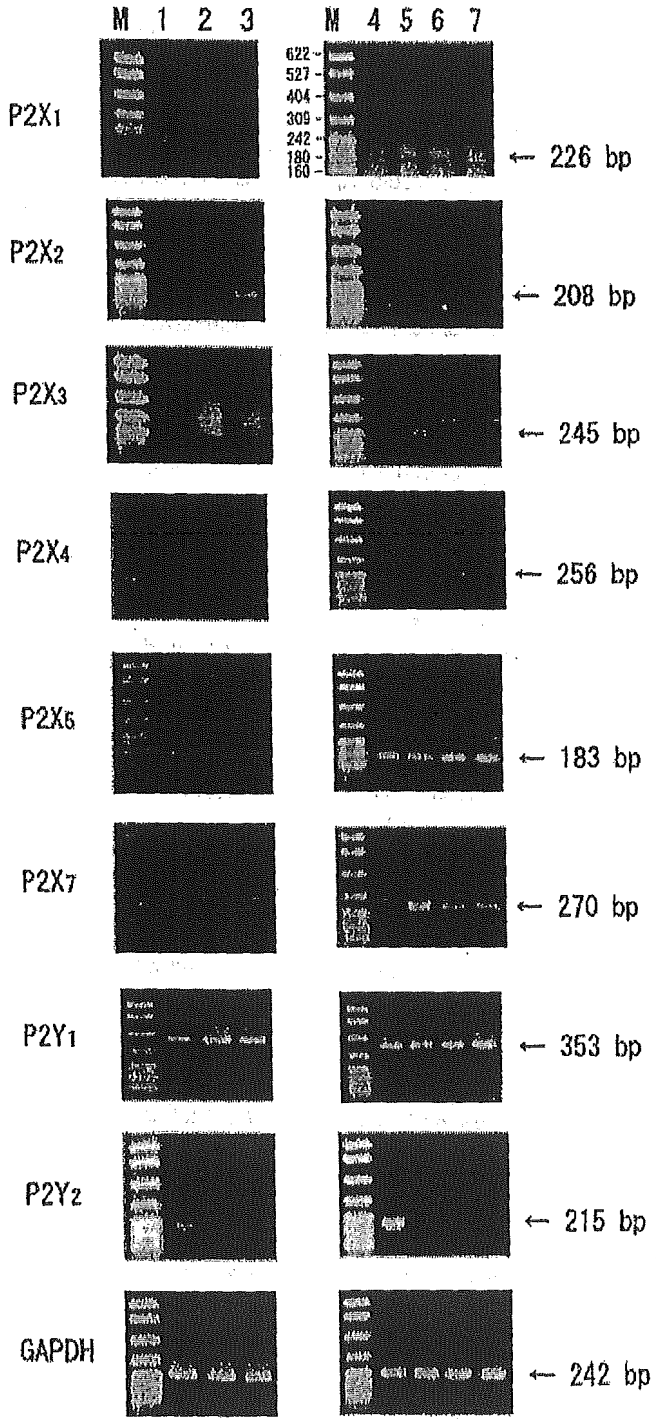

Figure 4
Changes in P2X and P2Y receptor subtype mRNA expressions in different conditions of normal human epidermal keratinocytes (NHEK). The left panels indicate that P2 receptor mRNA expression is affected by each culture condition. The right panels indicate that P2 receptor mRNA expression is affected while exposed to ATP and UVB radiation. Arrows indicate the PCR amplification products corresponding to P2X and P2Y receptor subtypes. M, DNA size markers; lane 1, proliferating subconfluent keratinocytes; lane 2, differentiating over-confluent keratinocytes; lane 3, differentiating over-confluent keratinocytes on addition of Ca (1.8 mM); lane 4, proliferating subconfluent keratinocytes; lane 5, proliferating subconfluent keratinocytes exposed to ATP (300 μM) for 6 h; lane 6, proliferating subconfluent keratinocytes exposed to UVB (60 mJ per cm^2); lane 7, proliferating subconfluent keratinocytes exposed to UVB (30 mJ per cm^2). Cytotoxicity was not found in any of the cell conditions (proliferating subconfluent keratinocytes; lanes 1 and 4, 1017 ± 52, n = 6, differentiating over-confluent keratinocytes; lane 2, 1152 ± 29, n = 6, differentiating over-confluent keratinocytes on addition of Ca; lane 3, 1173 ± 47, n = 6, proliferating subconfluent keratinocytes exposed to ATP for 6 h; lane 5, 1027 ± 43, n = 6, proliferating subconfluent keratinocytes exposed to UVB (60 mJ per cm^2); lane 6, 1025 ± 64, n = 6, proliferating subconfluent keratinocytes exposed to UVB (30 mJ per cm^2); lane 7, 1003 ± 41, n = 6).

of response to αβ-meATP and BzATP in differentiating overconfluent cells. On the other hand, the responses to ATP, UTP, and 2MeSADP decreased in the differentiated phase. Although the 2MeSADP-evoked $[Ca^{2+}]_i$ decreased in confluent cells, $P2Y_1$ expression remained unchanged. At this point however, we cannot distinguish the inconsistency between the expression level and Ca^{2+} response. Although 2MeSADP is also an agonist for $P2Y_{12}$, and $P2Y_{13}$, ADP, an agonist for $P2Y_1$, $P2Y_{12}$, and $P2Y_{13}$, elevated $[Ca^{2+}]_i$ in HaCaT keratinocytes but not in NHEK (Burrell *et al*, 2003). Thus, it is unlikely that these receptors are functional. Although the expression of $P2Y_2$ mRNA was downregulated at the differentiated phase, the expression of multiple $P2X_2$, $P2X_3$, $P2X_5$, and $P2X_7$ receptor subtype mRNA increased (Fig 4). Judging from the results of Ca^{2+} responses and RT-PCR, $P2X_3$ and $P2X_7$ receptor subtypes mainly function in the differentiated phase. The variation of multiple P2X receptor expression in cultured keratinocytes supports the notion that the $P2X_5$ and $P2X_7$ receptors are localized in the differentiated or terminal differentiated skin (Greig *et al*, 2003).

$P2X_3$ receptors are known to be selectively expressed in a subpopulation of small diameter sensory neurons (Chen *et al*, 1995; Lewis *et al*, 1995). $P2X_3$ receptors however, have been observed in nonneuronal cells, such as thymus (Glass *et al*, 2000) and urothelial cells (Sun and Chai, 2004). Stretching in bladder urothelial cells increased $P2X_3$ receptor expression and their expression was increased more in urothelial cells from patients with interstitial cystitis than that in control subjects (Sun and Chai, 2004). The epidermis could be an interface of the body and environment; hence, the P2X receptors may play a role as some kind of sensor against multiple environmental factors such as barrier disruption and UV radiation. $P2X_7$ receptors are known to be involved in ATP-induced apoptosis (Ferrari *et al*, 1997). $P2X_7$ receptors are likely to be part of the machinery of the end-stage terminal differentiation of keratinocytes (Greig *et al*, 2003). Extracellular ATP increased $P2X_1$, $P2X_2$, $P2X_3$, and $P2X_7$ receptors but not $P2X_4$, $P2X_5$ expression (Fig 4). UVB radiation also induces apoptosis in keratinocytes (Schwarz *et al*, 1995). In this study, $P2X_1$, $P2X_3$, and $P2X_7$ receptor expression, but not $P2X_2$ receptor expression, was augmented by UVB radiation. $P2X_4$, $P2X_5$, and $P2Y_1$ receptors expression however, was unaffected by ATP or UVB radiation. $P2Y_2$ receptor expression was downregulated by the application of ATP and UVB radiation. The downregulation of $P2Y_2$ receptors expression shows that extracellular ATP and UVB radiation inhibited proliferation. A high concentration of ATP inhibits proliferation and a low concentration of ATP promotes proliferation (Dixon *et al*, 1999; Greig *et al*, 2003).

We demonstrated that P2X receptors were nonselective cationic channels; on the other hand, the response to ATP mediated through P2Y receptors activated Cl^- conductance. Ca^{2+}-activated Cl channel and K channel contributed to the hyperpolarization induced by ATP, bradykinin, and histamine in HaCaT keratinocytes (Koegel and Alzheimer, 2001). Mauro *et al*, (1990) described that Cl^- conductance, increased by elevating extracellular Ca^{2+}, plays a role in the initiation of differentiation. Increases in $[Ca^{2+}]_i$ and phosphatidylinositol turnover because of the elevation of extracellular Ca^{2+} were important components of the signal for differentiation (Jaken and Yuspa, 1988; Hennings *et al*, 1989). These studies suggest the possibility that the intracellular Ca^{2+} released from IP_3-sensitive stores affects Cl^- conductance and resultantly leads to keratinocyte differentiation. With these studies as a background, it shall be assumed that Cl^- conductance via P2Y receptors also contributes to the initiation of differentiation. This ionic selectivity of P2 receptor subtypes may be associated with the localization in skin and contribute to the maintenance of homeostasis in skin.

Furthermore, a difference in the amount of released ATP or the localization of P2 receptors between normal healthy subjects and patients would be expected. ATP released from uroepithelial cells was higher in patients with interstitial cystitis than in controls (Sun *et al*, 2001). Since mechanical scratching has the potential to induce the release of a large amount of ATP release in atopic or psoriatic skin and leads to skin inflammation, it would appear that the purinergic signaling is clinically significant. The stimulation of ATP occurs throughout all stages, through proliferation, differentiation, and apoptosis. Regulation of P2 receptor subtypes is necessary in order to control ion influx and membrane potential, which helps maintain epidermal homeostasis.

In summary, we demonstrated the presence of functional multiple P2X receptors in NHEK, suggesting their important physiological role as an initial sensor for external stimuli. P2 receptor subtypes in keratinocytes would provide a basis to study the regulatory mechanisms underlying the differentiation and proliferation of keratinocytes.

Materials and Methods

Cells and cell culture NHEK (10 Strains of NHEK) were purchased from Kurabo (Osaka, Japan). NHEK were cultured in serum-free keratinocyte growth medium, consisting of Humedia-KB2 (Kurabo) supplemented with bovine pituitary extract (0.4% vol/vol), human recombinant epidermal growth factor (0.1 ng per mL), insulin (10 μg per mL), and hydrocortisol (0.5 μg per mL). The medium was replaced every 2–3 d. For the electrophysiological experiments, NHEK (passage 1–3 cells) were seeded onto collagen-coated glass coverslips and used within 4 d.

Electrophysiological recordings Membrane currents were measured using whole-cell clamp techniques (Hamill *et al*, 1981). Cells that were grown on collagen coated-cover slips were transferred to an experimental chamber of about 1 mL volume. The chamber was continuously perfused with an extracellular solution containing (in mM) NaCl 140, KCl 5.4, $CaCl_2$ 1.8, $MgCl_2$ 1.0, 10.0 *N*-2-hydroxyethylpiperazine-*N*′-2-ethanesulfonic acid (HEPES), 11.1 D-glucose (adjusted with NaOH to pH 7.4). Heat-polished patch pipettes had a tip resistance of 3–5 MΩ when filled with an intracellular solution containing 150 mM CsCl, 1 mM $MgCl_2$, 10 mM HEPES, and 5 mM-glycoletherdiamine *N*,*N*,*N*′,*N*′-tetraacetic acid (pH 7.2 with CsOH). Intracellular solution was supplemented with 0.3 mM guanosine 5′triphosphate (GTP) or 2 mM guanosine 5′-*O*-(2-thiodiphosphate) trilitium salt (GDPβS). To exclude the P2Y-activated current, GDPβS, an inhibitor of GTP-binding protein, was applied to the cells (Nakazawa, 1994). Three hundred millimolar KCl-agar bridge electrode was used as the reference electrode. Cell capacitance was compensated after the whole-cell mode was obtained. Cells were clamped at −60 mV. A step pulse between −100 and +40 mV was applied to the cell. Membrane currents were recorded with a patch-clamp amplifier (Axopatch 200B, Axon Instruments, Union City, California). Electrical signals were filtered

at 1 kHz. Current signals were stored in a personal computer and analyzed using pCLAMP 6.0 and Clampfit 6.0 software (Axon Instruments). The drugs were dissolved in the extracellular solution and applied to the cells by perfusion. The experiments were performed at room temperature (~25°C). TNP-ATP was purchased from Molecular Probes (Eugene, Oregon). All other chemicals were purchased from Sigma-Aldrich (St Louis, Missouri).

Ca^{2+} imaging in single keratinocyte NHEK were grown to approximately 60%–80% confluency (subconfluent), 100%–120% confluency (confluent), and 100%–120% confluency at 48 h post-treatment with 1.8 mM Ca^{2+} (confluent + Ca) on collagen-coated cover glass chambers (Nalge Nunc, Naperville, Illinois). Changes in $[Ca^{2+}]_i$ in single cell were measured by the fura-2 method as described by Grynkiewicz *et al* (1985) with minor modifications (Koizumi and Inoue, 1997). In brief, the culture medium was replaced with a balanced salt solution (BSS) of the following composition (mM): NaCl 150, KCl 5, $CaCl_2$ 1.8, $MgCl_2$ 1.2, HEPES 25, and D-glucose 10 (pH = 7.4). Cells were loaded with 5 μM fura-2 acetoxymethylester (fura-2AM) (Molecular Probes) at room temperature (~ 25°C) in BSS for 45 min, followed by a BSS wash and a further 15 min incubation to allow de-esterification of the loaded dye. The coverslip was mounted on an inverted epifluorescence microscope (IX70, TS Olympus, Tokyo, Japan), equipped with a 75 W xenon-lamp and band-pass filters of 340 and 380 nm wavelengths. The image data, recorded by a high-sensivity CCD (charge-coupled-device) camera (ORCA-ER, Hamamatsu Photonics, Hamamatsu, Japan) were regulated by a Ca^{2+} analyzing system (AQUACOSMOS/RATIO, Hamamatsu Photonics). In the Ca^{2+}-free experiments, Ca^{2+} was removed from the BSS and 1 mM EGTA was added. Nucleotides were dissolved in the BSS and the cells were exposed to it by method of perfusion. Data were represented as the ratio of fluorescence intensities of 340 and 380 nm.

The preparation for total RNA extraction and synthesis cDNA For RT-PCR studies, NHEK were grown in 10 cm collagen-coated dish (Asahi Techno Glass, Tokyo, Japan) to 60%–80% confluency (subconfluent), 100%–120% confluency (confluent), and 100%–120% confluency at 48 h post-treatment with 1.8 mM Ca^{2+} (confluent + Ca). Sixty to eighty percent confluency cells collected at 6 h post-treatment with UVB (30 and 60 mJ per cm^2) and ATP (300 μM). While using UV radiation, the medium was replaced by PBS (–). NHEK were exposed to UVB radiation from a bank of two Toshiba FL 20 SE sunlamps (Toshiba Electric, Tokyo, Japan). These tubes emit wavelengths between 280 and 340 nm, with a peak of 304 nm. Radiance was measured by a UV-Radiometer (Topcon, Tokyo, Japan). After exposing NHEK to radiation, the medium was added back to the dishes and NHEK were incubated at 37°C in 5% CO_2 for 6 h. ATP was applied with medium for 6 h at 37°C in 5% CO_2. Total RNA was isolated from all individual samples using ISOGEN (Nippon Gene, Osaka, Japan) according to the manufacturer's protocol. We synthesized cDNA from 1 μg of total RNA by the use of 200 U of M-MLV RT (Invitrogen, Carisbad, California) in 20 μL of reaction mixture containing 0.5 μg of oligo (dT) primer (Invitrogen), 50 mM Tris-HCl, pH 8.3, 75 mM KCl, 3 mM $MgCl_2$, 10 mM dithiothreitol, 0.25 mM dATP, 0.25 mM dTTP, 0.25 mM dGTP, 0.25 mM dCTP (Takara, Japan), and 50 U of ribonuclease inhibitor (Takara, Otsu, Japan) at 37°C for 1 h.

RT-PCR The amounts of P2 receptors and human GAPDH cDNA in samples were amplified by using an ABI PRISM 7700 sequence detector (Applied BioSystems, Foster City, California). The reaction mixture was as follows: PCR buffer, 3.5 mM $MgCl_2$, 0.2 μM forward primer, 0.2 μM reverse primer, 0.2 mM dNTP, and 1.25 U of AmpliTaq Gold DNA polymerase (Applied BioSystems). The PCR conditions were: 50°C for 2 min; 95°C for 10 min; 35 cycles of 95°C for 15 s; and 60°C for 1 min. Obtained DNA fragments by PCR

Table I. Primers list of P2 receptors and glyceraldehydes-3-phosphate dehydrogenase (GAPDH)

Gene	Primers (forward and reverse)	Accession number in GenBank	Product size (bp)
$P2X_1$	5′-CCAGCTTGGCTACGTGGTGCAAGA-3′	U45448	226
	5′-ACGGTAGTTGGTCCCGTTCTCCACAA-3′		
$P2X_2$	5′-CCCGAGAGCATAAGGGTCCACAAC-3′	AF190823	208
	5′-AATTTGGGGCCATCGTACCCAGAA-3′		
$P2X_3$	5′-CCCCTCTTCAACTTTGAGAAGGGA-3′	NM002559	245
	5′-GTGAAGGAGTATTTGGGGATGCAC-3′		
$P2X_4$	5′-CCTTCCCAACATCACCACTACTTACC-3′	U85975	256
	5′-AGGAGATACGTTGTGCTCAACGTC-3′		
$P2X_5$	5′-AGCACGTGAATTGCCTCTGCTTAC-3′	AF016709	183
	5′-ATCAGACGTGGAGGTCACTTTGCTC-3′		
$P2X_6$	5′-ATGGCCCTGTCCAAGTTCTGACAC-3′	AF065385	140
	5′-TGTTGCCTCATCCTTGCTTTCGCT-3′		
$P2X_7$	5′-CTGCTCTCTTGAACAGTGCCGAAA-3′	Y09561	270
	5′-AGTGATGGAACCAACGGTCTAGGT-3′		
$P2Y_1$	5′-ACCTCAGACGAGTACCTGCGAAGT-3′	NM002563	353
	5′-AGAATGGGGTCCACACAACTGTTGAG-3′		
$P2Y_2$	5′-GTGTCTGGGCGTCTTACGACCTCT-3′	NM176072	215
	5′-GCATGACTGAGCTGTAGGCCACGAA-3′		
GAPDH	5′-GAAGGTGAAGGTCGGAGTC-3′	NM002046	242
	5′-GAAGATG GTGATGGGATTTC-3′		

were separated in 1% agarose in Tris-borate buffer containing 0.25 μg per mL ethidium bromide. The gel was visualized by ultraviolet B radiation. PCR primers were designed using Genetyx Software program (GENETYX, Japan). The primers (forward, reverse, accession number, and product size) are shown in Table I.

Cell viability The applied condition of ATP for 6 h (300 μM) and the condition of 6 h post-treatment with UVB (30 and 60 mJ per cm^2) on the cytotoxicity were assessed using an AlamarBlue assay (Alamar Biosciences, Camarillo, California), according to the manufacturer's protocol. The fluorescence intensities were determined at 544 and 590 nm.

Statistics Data represent the mean ± SD. Statistical differences between two groups were determined by a two-tailed Student's test. In the case of more than two groups, differences were analyzed by analysis of variance (ANOVA test) and Scheffe's test. $p < 0.05$ was considered to be statistically significant.

We are grateful to Ms T Obama (Division of Biosignaling, National Institute of Health Sciences) for her skillful culturing of cells.

DOI: 10.1111/j.0022-202X.2005.23683.x

Manuscript received September 11, 2004; revised December 17, 2004; accepted for publication December 21, 2004

Address correspondence to: Kaori Inoue, PhD, Shiseido Research Center, 2-12-1 Fukuura, Kanazawa-ku, Yokohama 236-8643, Japan. Email: kaori.inoue@to.shiseido.co.jp

References

Bo X, Jiang L-H, Wilson HL, Kim M, Burnstock G, Surprenant A, North RA: Pharmacological and biophysical properties of the human $P2X_6$ receptor. Mol Pharmacol 63:1407–1416, 2003

Burnstock G, Wood JN: Purinergic receptors: Their role in nociception and primary afferent neurotransmission. Curr Opin Neurobiol 6:526–532, 1996

Burrell HE, Bowler WB, Gallagher JA, Sharpe GR: Human keratinocytes express multiple P2Y-receptors: Evidence for functional P2Y1, P2Y2, and P2Y4 receptors. J Invest Dermatol 120:440–447, 2003

Chen CC, Akopian AN, Sivilotti L, Colquhoun D, Burnstock G, Wood JN: A P2X purinoceptor expressed by a subset of sensory neurons. Nature 377: 428–431, 1995

Cook SP, McCleskey EW: Cell damage excites nociceptors through release of cytosolic ATP. Pain 95:41–47, 2002

Denda M, Inoue K, Fuziwara S, Denda S: P2X purinergic receptor antagonist accelerates skin barrier repair and prevents epidermal hyperplasia induced by skin barrier disruption. J Invest Dermatol 119:1034–1040, 2002

Dixon CJ, Bowler WB, Littlewood-Evans A, Dillon JP, Bilbe G, Sharpe GR, Gallagher JA: Regulation of epidermal homeostasis through $P2Y_2$ receptors. Br J Pharmacol 127:1680–1686, 1999

Evans RJ, Surprenant A: P2X receptors in autonomic and sensory neurons. Semin Neurosci 8:217–223, 1996

Ferguson DR, Kennedy I, Burton TJ: ATP is released from rabbit urinary bladder epithelial cells by hydrostatic pressure changes—a possible sensory mechanism? J Physiol 505:503–511, 1997

Ferrari D, Chiozzi P, Falzoni S, Dal Susino M, Collo G, Buell G, Di Virgilio F: ATP-mediated cytotoxicity in microglial cells. Neuropharmacol 36:1295–1301, 1997

Glass R, Townsend-Nichols A, Burnstock G: P2 receptors in the thymus: Expression of P2X and P2Y receptors in adult rats, an immunohistochemical and *in situ* hybridisation study. Cell Tissue Res 300:295–306, 2000

Greig AVH, Linge C, Terenghi G, McGrouther A, Burnstock G: Purinergic receptors are part of a functional signaling system for proliferation and differentiation of human epidermal keratinocytes. J Invest Dermatol 120: 1007–1015, 2003

Grubb BD, Evans RJ: Characterization of cultured dorsal root ganglion neuron P2X receptors. Eur J Neurosci 11:149–154, 1999

Grynkiewicz G, Poenie M, Tsien RY: A new generation of Ca^{2+} indicators with greatly improved fluorescence properties. J Biol Chem 260:3440–3450, 1985

Hamill OP, Marty A, Neher E, Sakmann B, Sigworth FJ: Improved patch-clamp techniques for high-resolution current recording from cells and cell-free membrane patches. Pflugers Arch 391:85–100, 1981

Hansen M, Boitano S, Dirksen ER, Sanderson MJ: Intercellular calcium signaling induced by extracellular adenosine 5′-triphosphate and mechanical stimulation in airway epithelial cells. J Cell Sci 106:995–1004, 1993

Hennings H, Kruszewski FH, Yuspa SH, Tucker RW: Intracellular calcium alterations in response to increased external calcium in normal and neoplastic keratinocytes. Carcinogenesis 10:777–780, 1989

Jaken Y, Yuspa SH: Early signals for keratinocyte differentiation: Role of Ca^{2+}-mediated inositol lipid metabolism in normal and neoplastic epidermal cells. Carcinogenesis 9:1033–1038, 1988

Jiang L-H, Mackenzie AB, North RA, Surprenant A: Brilliant Blue G selectively blocks ATP-gated rat $P2X_7$ receptors. Mol Pharmacol 58:82–88, 2000

Koegel H, Alzheimer C: Expression and biological significance of Ca^{2+}-activated ion channels in human keratinocytes. FASEB 15:145–154, 2001

Koizumi S, Fujishita K, Inoue K, Shigemoto-Mogami Y, Tsuda M, Inoue K: Ca^{2+} waves in keratinocytes are transmitted to sensory neurons: The involvement of extracellular ATP and P2Y2 receptor activation. Biochem J 380: 329–338, 2004

Koizumi S, Inoue K: Inhibition by ATP of calcium oscillations in rat cultured hippocampal neurones. Br J Pharmacol 122:51–58, 1997

Lee WK, Choi SW, Lee HR, Lee EJ, Lee KH, Kim HO: Purinoceptor-mediated calcium mobilization and proliferation in HaCaT keratrinocytes. J Dermatol Sci 25:97–105, 2001

Lewis C, Neidhart S, Holy C, North RA, Buell G, Surprenant A: Coexpression of $P2X_2$ and $P2X_3$ receptor subunits can account for ATP-gated currents in sensory neurons. Nature 377:432–435, 1995

Mauro TM, Pappone PA, Isseroff RR: Extracellular calcium affects the membrane currents of cultured human keratinocytes. J Cell Physiol 143:13–20, 1990

Milner P, Bodin P, Loesch A, Burnstock G: Rapid release of endothelin and ATP from isolated aortic endothelial cells exposed to increased flow. Biochem Biophys Res Commun 170:649–656, 1990

Nakazawa K: Modulation of the inhibitory action of ATP on acetylcholine-activated current by protein phosphorylation in rat sympathetic neurons. Pflugers Arch 427:129–135, 1994

Norenberg W, Illes P: Neuronal P2X receptors: Location and functional properties. Naunyn-Schmiedeberg's Arch Pharmacol 362:324–339, 2000

North RA, Surprenant A: Pharmacology of cloned P2X receptors. Annu Rev Pharmacol Toxicol 40:563–580, 2000

Pillai S, Bikle DD: Adenosine triphosphate stimulates phosphoinositide metabolism, mobilizes intracellular calcium, and inhibits terminal differentiation of human epidermal keratinocytes. J Clin Invest 90:42–51, 1992

Schwarz A, Bhardwaj R, Aragane Y, *et al*: Ultraviolet-B-induced apoptosis of keratinocytes: Evidence for partial involvement of tumor necrosis factor-α in the formation of sunburn cells. J Invest Dermatol 104:922–927, 1995

Sun Y, Chai TC: Up-regulation of $P2X_3$ receptor during stretch of bladder urothelial cells from patients with interstitial cystitis. J Urol 171:448–452, 2004

Sun Y, Keay S, De Deyne PG, Chai TC: Augmented stretch activated adenosine triphosphate release from bladder uroepithelial cells in patients with interstitial cystitis. J Urol 166:1951–1956, 2001

Thorne PR, Housley GD: Purinergic signaling in sensory systems. Semin Neurosci 8:233–246, 1996

Ueno S, Koizumi S, Inoue K: Characterization of Ca^{2+} influx through recombinant P2X receptor in C6BU-1 cells. Br J Pharmacol 124:1484–1490, 1998

Journal of Neurochemistry, 2005, 93, 1383–1392 doi:10.1111/j.1471-4159.2005.03097.x

Long-lasting change in brain dynamics induced by methamphetamine: enhancement of protein kinase C-dependent astrocytic response and behavioral sensitization

Minoru Narita,* Mayumi Miyatake,* Masahiro Shibasaki,* Makoto Tsuda,† Schuichi Koizumi,‡ Michiko Narita,* Yoshinori Yajima,* Kazuhide Inoue† and Tsutomu Suzuki*

**Department of Toxicology, Hoshi University School of Pharmacy and Pharmaceutical Sciences, Tokyo, Japan*
†Division of Biosignaling, ‡Division of Pharmacology, National Institute of Health Sciences, Tokyo, Japan

It is well known that long-term exposure to psychostimulants induces neuronal plasticity. Recently, accumulating evidence suggests that astrocytes may actively participate in synaptic plasticity. In this study, we found that *in vitro* treatment of cortical neuron/glia co-cultures with either methamphetamine (METH) or morphine (MRP) caused the activation of astrocytes via protein kinase C (PKC). Purified astrocytes were markedly activated by METH, whereas MRP had no such effect. METH, but not MRP, caused a long-lasting astrocytic activation in cortical neuron/glia co-cultures. Furthermore, MRP-induced behavioral sensitization to hyper-locomotion was reversed by 2 months of withdrawal following intermitted MRP administration, whereas behavioral sensitization to METH-induced hyper-locomotion was maintained even after 2 months of withdrawal. Consistent with this cell culture study, *in vivo* treatment with METH, which was associated with behavioral sensitization, caused a PKC-dependent astrocytic activation in the cingulate cortex and nucleus accumbens of mice. These findings provide direct evidence that METH induces a long-lasting astrocytic activation and behavioral sensitization through the stimulation of PKC in the rodent brain. In contrast, MRP produced a reversible activation of astrocytes via neuronal PKC and a reversibility of behavioral sensitization. This information can break through the definition of drugs of abuse and the misleading of concept that morphine produces a long-lasting neurotoxicity.

Keywords: astrocyte, synaptic plasticity, psychostimulant, opioid, protein kinase C, neuron–glia communication.
J. Neurochem. (2005) **93**, 1383–1392.

Glial cells, including astrocytes, microglia and oligodendrocytes, are the most numerous type of brain cells, and their roles in providing structural, metabolic and trophic support to neurons are well established (Kettenmann and Ransom 1995; Bezzi and Volterra 2001). Over the past decade, an increasing number of observations have progressively challenged the classical view that glial cells only serve passive supportive functions in mammalian CNS. For example, one glial type, oligodendrocyte precursor cells has been shown to receive direct synaptic input from neurons in the hippocampus (Bergles *et al.* 2000), and another glial cell type, astrocyte, releases glutamate rapidly in response to physiological increases in intracellular Ca^{2+} concentration ($[Ca^{2+}]_i$) (Parpura and Haydon 2000).

Astrocytes are a subpopulation of glial cells that control brain homeostasis to meet neuronal metabolic demands. Furthermore, astrocytes have a large variety of receptors for neurotransmitters and hormones, including dopamine receptor (Khan *et al.* 2001) and glutamate receptor (Nedergaard *et al.* 2002), which are coupled to various intracellular signaling cascades (Haydon 2001). Astrocytes are known to exhibit a form of excitability and communication based on changes in $[Ca^{2+}]_i$, which can be stimulated by neuronal synaptic activity (Parri *et al.* 2001). More recently, astrocytes have been reported to promote axonal extension and neuronal

Received September 1, 2004; revised manuscript received December 4, 2004; accepted January 17, 2005.

Address correspondence and reprint requests to Minoru Narita and Tsutsomu Suzuki, Department of Toxicology, Hoshi University School of Pharmacy and Pharmaceutical Sciences, 2-4-41 Ebara, Shinagawaku, Tokyo 142-8501, Japan.
E-mail: narita@hoshi.ac.jp and suzuki@hoshi.ac.uk.

Abbreviations used: NPC-15437, *S*-2,6-diamino-*N*-[(1-[1-oxotridecyl]-2-piperidinyl)methyl]hexamide dihydorochloride; BSS, basal salt saline; CHE, chelerythrine chloride; DA, dopamine; GFAP, glial fibrillary acidic protein; GLU, glutamate; METH, methamphetamine; MRP, morphine; PFA, paraformaldehyde; PBS, phosphate-buffered saline; PKC, protein kinase C; p-PKC, phosphorylated-protein kinase C.

© 2005 International Society for Neurochemistry,

migration, whereas astrocyte-derived cues also play a critical role in the pathological process by forming boundaries and retarding axonal outgrowth (Powell *et al.* 2001).

It has been documented recently that astrocytes in the neostriatum show hypertrophy and proliferation upon treatment with methamphetamine (METH) at neurotoxic doses in mice (Pu and Vorhees 1995). Astrocytic morphological changes can also be induced by the administration of cocaine in mice (Fattore *et al.* 2002). These findings indicate that astrocytes may play an important role in the development of dependence on psychostimulants. However, relatively little is known about the mechanism that underlies psychostimulant-induced astrocytic responses, even if astrocytes are considered to play a critical role in long-term synaptic plasticity in the CNS (Ullian *et al.* 2001; Song *et al.* 2002). In the present study, we investigated the mechanism of METH-induced astrocytic activation in cultured cortical astrocytes and cortical neuron/glia co-cultures. We also documented whether morphine (MRP) could directly regulate astrocytic responses to cultures.

METH and cocaine are strongly addictive psychostimulants that dramatically affect the CNS, and they are highly abused drugs worldwide. Abuse of psychostimulants leads to the development of psychotic symptoms that resemble those of paranoid schizophrenia (Synder 1974). In rodents, it has been shown consistently that repeated exposure to psychostimulants results in a progressive and enduring enhancement in the motor stimulant effect elicited by a subsequent drug challenge, which termed behavioral sensitization (Vanderschuren and Kalivas 2000). Accumulating evidence suggests that the behavioral sensitization induced by psychostimulants may be accompanied by long-lasting neural plasticity (Robinson and Kolb 1999) that may involve structural modifications in the dopaminergic (Steketee 2003) and/or glutamatergic system (Sripada *et al.* 2001). Here we report for the first time that chronic treatment with METH causes a long-lasting PKC-dependent behavioral sensitization related to the enhanced astrocytic responses, whereas MRP produces a reversible behavioral sensitization.

Materials and methods

The present studies were conducted in accordance with the Guide for Care and Use of Laboratory Animals adopted by the Committee on Care and Use of Laboratory Animals of Hoshi University School of Pharmacy and Pharmaceutical Sciences, which is accredited by the Ministry of Education, Culture, Sports, Science and Technology of Japan.

Tissue processing

Purified cortical astrocytes were grown as follows: cerebral cortices were obtained from newborn ICR mice (Tokyo Laboratory Animals, Tokyo, Japan), minced, and treated with trypsin (0.025%, Invitrogen, Carlsbad, CA, USA) dissolved in phosphate-buffered saline (PBS) solution containing 0.02% L-cysteine (Sigma-Aldrich, St. Louis, MO, USA) monohydrate, 0.5% glucose (Wako Pure Chemicals, Osaka, Japan) and 0.02% bovine serum albumin (Wako Pure Chemicals). After enzyme treatment at 37°C for 15 min, cells were dispersed by gentle agitation through a pipette and plated on a flask. One week after seeding in Dulbecco's modified Eagle's medium (DMEM, Invitrogen) supplemented with 5% precolostrum newborn calf serum (FBS, Invitrogen), 5% heat-inactivated (56°C, 30 min) horse serum (HS, Invitrogen), 10 U/mL penicillin and 10 μg/mL streptomycin in a humidified atmosphere of 95% air and 5% CO_2 at 37°C, the flask was shaken for 12 h at 37°C to remove nonastrocytic cells. The cells were seeded at a density of 1×10^5 cells/cm^2. The cells were maintained for 3–10 days in DMEM supplemented with 5% FBS, 5% HS, 10 U/mL penicillin and 10 μg/mL streptomycin in a humidified atmosphere of 95% air and 5% CO2 at 37°C.

Cortical neuron/glia co-cultures were grown as follows: cerebral cortex was obtained from newborn ICR mice (Tokyo Laboratory Animals Science), minced, and treated with papain (9 U/mL, Worthington Biochemical, Lakewood, NJ, USA) dissolved in PBS solution containing 0.02% L-cysteine monohydrate, 0.5% glucose and 0.02% bovine serum albumin. After enzyme treatment at 37°C for 15 min, cells were seeded at a density of 2×10^6 cells/cm^2. The cells were maintained for 7 days in DMEM supplemented with 10% FBS, 10 U/mL penicillin and 10 μg/mL streptomycin. On day 8, the cells were treated with drugs.

Drug treatment and immunohistochemistry

At day 3–7 *in vitro*, the cells were treated with either normal medium, methamphetamine hydrochloride (METH, 0.01–1000 μM, Dainippon Pharmaceutical, Osaka, Japan), a selective protein kinase C (PKC) inhibitor, chelerythrine chloride (CHE, 10 nM, Sigma-Aldrich) + METH (1–100 μM), morphine hydrochloride (MRP, 1–1000 μM, Sankyo, Tokyo, Japan) or MRP (1–100 μM) + CHE (10 nM). The treatments lasted for 1–3 days. The cells were then identified by immunofluorescence using rabbit anti-glial fibrillary acidic protein antibody (GFAP, 1 : 1000; Chemicon International, Inc., Temecula, CA, USA), mouse anti-GFAP antibody (1 : 1000, Chemicon, International, Inc.), rabbit anti-phosphorylated-protein kinase C antibody (p-PKC, 1 : 400; Cell Signaling Technology Inc., Beverly, MA, USA), or rabbit anti-cleaved caspase-3 antibody (1 : 100, Cell Signaling Technology Inc., Beverly, MA, USA), followed by incubation with Alexa 488-conjugated goat anti-rabbit antibody (1 : 4000) or Alexa 546-conjugated goat anti-rabbit antibody (1 : 4000) for GFAP, Alexa 488-conjugated goat anti-rabbit antibody (1 : 1000) for p-PKC, and Alexa 488-conjugated goat anti-rabbit antibody (1 : 10000) for cleaved caspase-3. Images were collected using a Radiance (2000) laser-scanning microscope (Bio-Rad, Richmond, CA, USA).

The density of GFAP-like immunoreacivity was measured with a computer-assisted system (NIH IMAGE). The upper and lower threshold density ranges were adjusted to encompass and match the immunoreactivity to provide an image with immunoreactive material appearing in black pixels, and non-immunoreactive material as white pixels. The area and density of pixels within the threshold value representing immunoreactivity were calculated.

Evaluation of astrocytic stellation

In order to evaluate the astrocytic stellation, purified cortical astrocytes were cultured on 24-well plates and treated with METH

(0.01–100 μM) or METH (1–100 μM) + CHE (10 nM) for 1–3 days. The cells were fixed in 4% paraformaldehyde and stained with cresyl violet (0.1%, ICN Biomedicals, Aurora, OH, USA) to determine the percentage of stellate cells in cultures. Cells with processes longer than their perinuclear diameters were defined as stellate cells. Stained cells were mounted on glass slides and viewed under transmitted light using a microscope with a 10× objective lens (IX 70, Olympus Optical, Tokyo, Japan). For each coverslips, four randomly chosen fields were counted (about 170 cells in each field), and the percentage of stellate cells was determined. Each experimental condition was repeated from four independent culture preparations. The percentage of stellate cells was expressed as average ± SE. Student's *t*-test was used for statistical analysis.

Confocal Ca^{2+} imaging

Purified cortical astrocytes were loaded with 10 μM fluo-3 acetoxymethyl ester (Dojindo Molecular Technologies, Inc., Gaithersburg, MD, USA) for 90 min at room temperature. After a further 20–30 min of de-esterification with the acetoxymethyl ester, the coverslips were mounted on a microscope equipped with a confocal Ca^{2+} imaging system (Radiance 2000, Bio-Rad). Fluo-3 was excited with the 488 nm line of an argon-ion laser and the emitted fluorescence was collected at wavelengths > 515 nm, and average baseline fluorescence (F_0) of each cells was calculated. To compensate for the uneven distribution of fluo-3, self-ratios were calculated (Ratio: $R_s = F/F_0$).

Dopamine (1–100 μM, Sigma-Aldrich) or glutamate (1–100 μM, Sigma-Aldrich) was perfused for 30 sec at 5 mL/min at room temperature in cultured cortical astrocytes followed by superfusion of basal salt saline (BSS, pH 7.4) containing 150 mM NaCl, 5.0 mM KCl, 1.8 mM $CaCl_2$, 1.2 mM $MgCl_2$, 25 mM *N*-2-hydroxyethylpiperazine-*N'*-2-ethaneslufonic acid and 10 mM D-glucose.

Locomotor assay for METH and MRP

Male ICR mice (20–25 g) were housed at a room temperature of 23 ± 1°C with a 12-h light : 12-h dark cycle (lights on 08:00–20:00). Food and water were available *ad libitum*.

The locomotor activity of mice was measured by an ambulometer (ANB-M20, O'Hara, Tokyo, Japan) as described previously (Narita *et al.* 1993). Briefly, a mouse was placed in a tilting-type round activity cage of 20 cm in diameter and 19 cm in height. Any slight tilt of the activity cage caused by horizontal movement of the animal was detected by micro-switches. Total activity counts in each 10-min segment were automatically recorded for 30 min prior to the injections and for 180 min following METH administration.

According to previous reports (Kuribara 1996; Narita *et al.* 2002), a repeated injection paradigm was used in which animals were treated with an injection of METH (2 mg/kg, s.c.) or MPR (10 mg/kg, s.c.) every 96 h to induce sensitization to METH- or MRP-induced hyper-locomotion. Total activity was counted for 3 h after each treatment.

To investigate the implication of PKC in the development of sensitization to METH-induced hyper-locomotion, mice were pretreated with saline or a selective PKC inhibitor *S*-2,6-diamino-*N*-[(1-[1-oxotridecyl]-2-piperidinyl)methyl]hexamide dihydorochloride (NPC-15437: 1 mg/kg, s.c., Sigma-Aldrich) 30 min prior to METH (2 mg/kg, s.c.) treatment.

Immunohistochemistry using brain-slice sections

Twenty-four hours after the last METH treatment, animals were deeply anesthetized with sodium pentobarbital (50 mg/kg, i.p.) and perfused transcardially with 4% paraformaldehyde (PFA) in 0.1 M PBS. Then, the brains were removed quickly after perfusion and thick coronal section of the forebrain including the caudate putamen, nucleus accumbens, and cingulate cortex region was initially dissected using brain blocker. The coronal section of the midbrain was post-fixed in 4% PFA for 2 h. After the brains were permeated with 20% sucrose for 2 days and 30% sucrose for 2 days, they were frozen in an embedding compound (Sakura Finetechnical, Tokyo, Japan) on isopentane using liquid nitrogen and stored at −30°C until used. Frozen coronal sections (8 μm) were cut in a cryostat, and thaw-mounted on poly-L-lysine-coated glass slides.

Each primary antibody was diluted in 0.01 M PBS containing 10% normal horse serum [1 : 10 GFAP (Nichirei Co., Tokyo, Japan)] and was incubated twice overnight at 4°C. The antibodies were then rinsed and incubated with each secondary antibody for 2 h at room temperature. For each labeling, Alexa 488-conjugated goat anti-rabbit antibody for GFAP was diluted 1 : 1200 in PBS containing 10% NHS.

Statistical analysis

The data are presented as the mean ± SEM. The statistical significance of differences between groups was assessed by an analysis of variance (ANOVA) followed by Dunnett's multiple comparisons test or Student's *t*-test.

Results

METH-induced astrocytic activation

Treatment with METH (10 μM) for 3 days caused a robust activation of cultured cortical astrocytes, as detected by a stellate morphology and an increase in the level of GFAP-like immunoreactivity (GFAP-IR) compared to that in normal medium-treated cells (Fig. 1A). As shown in Fig. 1B, treatment with METH (1–100 μM) for 1–3 days significantly increased the number of stellate astrocytes in cultured cortical astrocytes. Although 1 day treatment with METH caused a significant increase in stellate astrocytes in cultured astrocytes, 3 day treatment with METH (10–100 μM) showed a drastic increase in stellate astrocytes. In addition, this activation of astrocytes was partially reversed by treatment with the specific protein kinase C (PKC) inhibitor chelerythrine chloride (CHE, Fig. 1), indicating the possible implication of PKC in this event. Immunohistochemical staining with an anti-phosphorylated PKC (p-PKC) antibody confirmed that treatment with METH increased the immunoreactiviy of p-PKC in astrocytes (Fig. 1D). These results suggest that astrocytic PKC is involved in METH-induced astrocytic activation (Fig. 1C). Treatment with METH (10–100 μM) for 3 days also caused a robust astrocyte activation in cortical neuron/glia co-cultures, and this activation was reversed by cotreatment with CHE (Fig. 2).

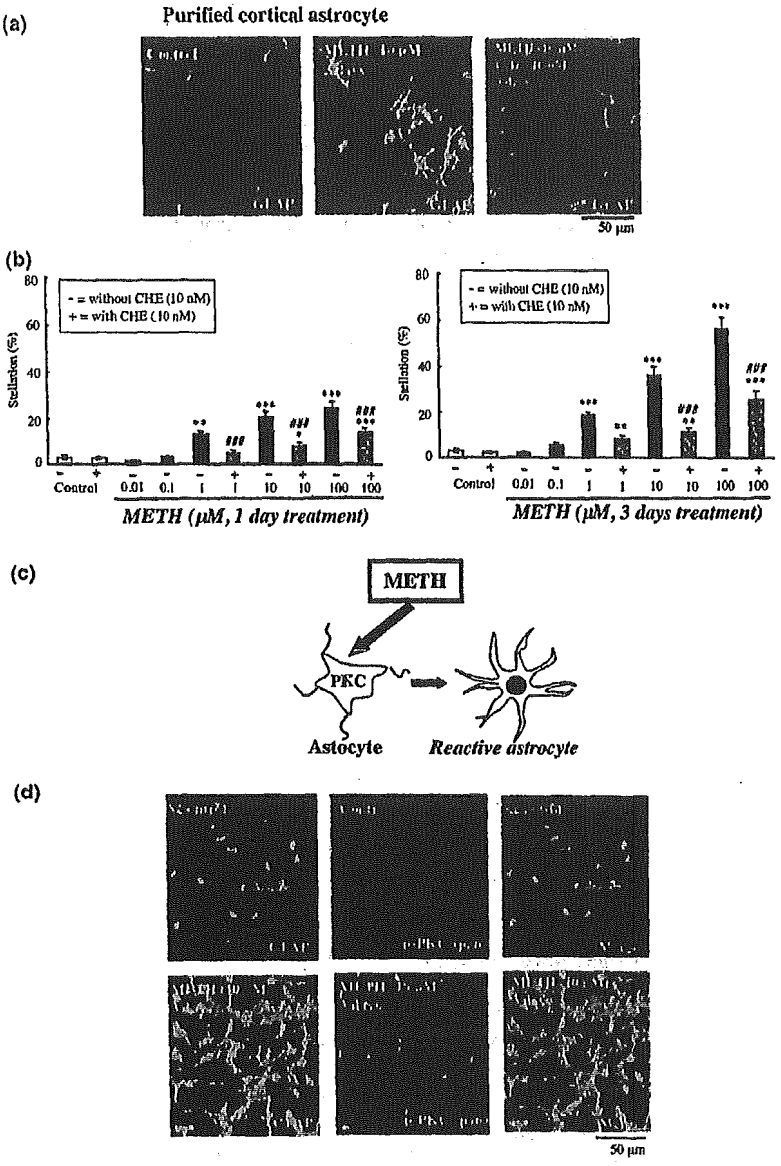

Fig. 1 Treatment with methamphetamine (METH) causes astrocytic activation in purified cortical astrocytes. (a) Purified cortical astrocytes were incubated with normal medium, METH (10 μM) or METH + chelerythrine (CHE, 10 nM) for 3 days. The cells were stained with a rabbit polyclonal antibody to GFAP. (b) Purified cortical astrocytes were incubated with normal medium, METH (0.01–100 μM) or METH (1–100 μM) + CHE (10 nM) for 1–3 days. Astrocytic activation as shown by a stellate morphology with processes longer than their perinuclear diameters was evaluated. Data represent the mean ± SEM of 139–250 cells from four separate observations. $^{**}p < 0.01$ and $^{***}p < 0.001$; control, $\#\#\#p < 0.001$; vs. cells without CHE. (c) Proposed scheme showing the mechanism of METH-induced atrocytic activation. (d) The green labeled for p-PKC (pan) stained with a rabbit polyclonal antibody and the red labeled for GFAP stained with a mouse polyclonal antibody are mostly overlapped as yellow in METH-treated astrocytes.

We next investigated whether treatment with METH could induce any functional changes in astrocytes. Astrocytes are known to express a variety of neurotransmitters and/or hormone receptors, including dopamine (DA) and glutamate (GLU) receptors. As shown in Fig. 3 2, either DA (1–100 μM) or GLU (1–100 μM) produced a transient increase in the intracellular calcium concentration ($[Ca^{2+}]_i$) in cultured cortical astrocytes. The Ca^{2+} responses to DA and GLU in astrocytes were significantly enhanced by 3 days of treatment with METH (10 μM, 3 days).

Morphine-induced astrocytic activation

Opioid agonists such as morphine (MRP) modulate several physiological processes including a rewarding effect by stimulating opioid receptors. To compare its effects with those of METH, we investigated the effect of MRP in astrocytes. Unlike METH, treatment with MRP (1–1000 μM) for 1–3 days did not produce morphological changes in the activation of purified cortical astrocytes (Figs 4a and b). In contrast to MRP treatment in purified astrocytes, treatment with MRP (10–100 μM) for 3 days activated GFAP-positive astrocytes in cortical neuron/glia co-cultures (Figs 4c and d), and this activation was partially attenuated by CHE (10 nM).

Different maintenance of METH- and MRP-induced astrocytic activation

We next investigated the difference between METH and MRP in the maintenance of astrocytic activation. As shown

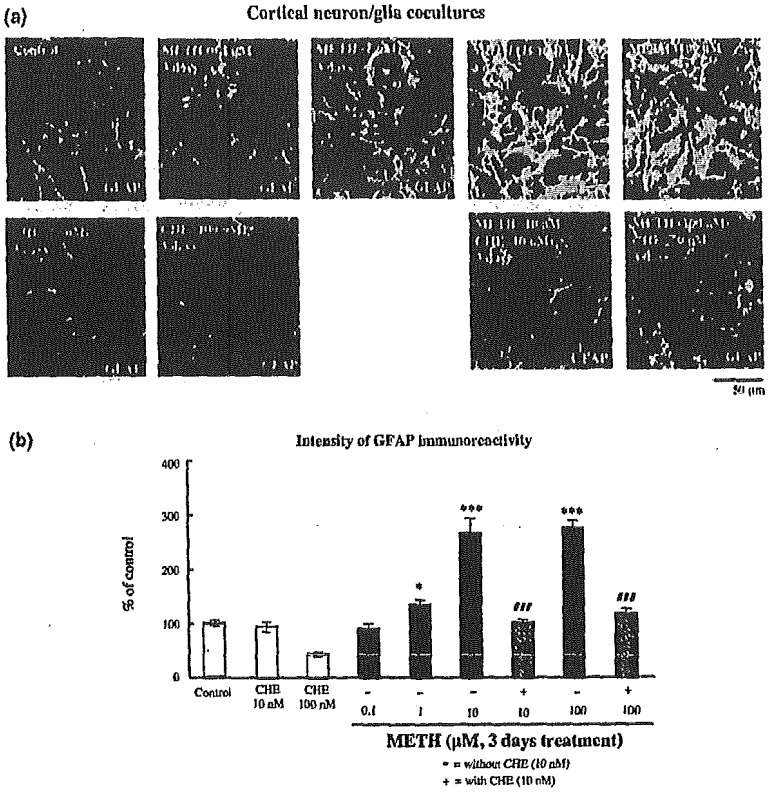

Fig. 2 Treatment with methamphetamine (METH) for 3 days causes astrocytic activation in cortical neuron/glia co-cultures. (a) Cortical neuron/glia co-cultures were with normal medium, METH (0.1–100 μM) or METH (1–100 μM) + CHE (10 nM) for 3 days. The cells were stained with a rabbit polyclonal antibody to GFAP. (b) The density of GFAP-like immunoreactivity of each image was measured using NIH IMAGE. The level of GFAP like immunoreactivity on MEHT- and METH + CHE-treated cells is expressed as a percent increase (mean ± SEM) with respect to that on control cells. $^{*}p < 0.05$, $^{***}p < 0.001$; vs. control cells. $\#\#\#p < 0.001$; vs. METH-treated cells.

in Fig. 5a, treatment with METH (10 μM) for 1–3 days caused the activation of GFAP-positive astrocytes in cortical neuron/glia co-cultures. The METH-contained medium was then switched to normal medium, and the cells were cultured for additional 2 days. It is of interest to note that the METH-induced increase in the level of GFAP-IR still remained after an additional 2 days of cultured with normal medium. Treatment with MRP (10 μM) for 1–3 days also caused the activation of GFAP-positive astrocytes in cortical neuron/glia co-cultures (Fig. 5b). The MRP-containing medium was then switched to normal medium, and the cells were cultured for additional 2 days. Unlike METH, the MRP-induced increase in the level of GFAP-IR was reversed after an additional 2 days of cultured with normal medium.

Long-lasting maintenance of behavioral sensitization to METH, but not MRP

The repeated administration of psychostimulant drugs results in a progressive and enduring elevation in the motor response elicited, which may be accompanied by a long-lasting neural plasticity. Therefore, we hypothesized that the psychostimulant-induced astrocytic activation may be related to behavioral sensitization. Based on the data and the hypothesis presented above, we next investigated whether repeated *in vivo* treatment with METH could cause a long-lasting maintenance of behavioral sensitization to METH-induced hyper-locomotion.

To clarify the development of sensitization to METH- or MRP-induced hyper-locomotion, mice were given five treatments [METH (2 mg/kg, s.c.) or MRP (10 mg/kg, s.c.)] every 96 h. As shown in Fig. 6, repeated injection of either METH or MRP produced a progressive elevation of the METH- or MRP-induced locomotor-enhancing effect, indicating the development of sensitization to METH- or MRP-induced hyper-locomotion ($p < 0.01$, first session vs. fifth session). Intriguingly, the METH-induced sensitization to hyper-locomotion was maintained even after 2 months withdrawal following intermitted METH administration (Fig. 6a). However, the MRP-induced sensitization was reversed by 2 months withdrawal following intermitted MRP administration (Fig. 6b).

METH-induces neuronal cell death

METH has been recognized as a drug of abuse that induces nerve terminal degeneration and neuronal apoptosis in the mammalian brain (Jiménez *et al.* 2004). We therefore investigated whether *in vitro* treatment with high concentration of METH or MRP could induce neuronal cell death. As shown in Fig. 7, treatment with

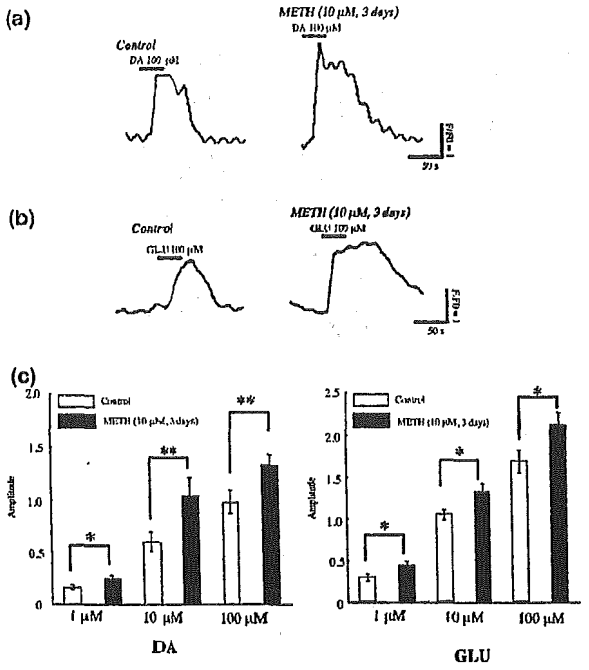

Fig. 3 The Ca^{2+} responses to dopamine and glutamate in astrocytes were significantly enhanced by 3 days of treatment with METH. (a) Traces show the dopamine (DA, 100 μM)-evoked increase in the intracellular Ca^{2+} concentration in control and METH-treated astrocytes. (b) Traces show the glutamate (GLU, 100 μM)-evoked increase in the intracellular Ca^{2+} concentration in control and METH-treated astrocytes. (c) The Ca^{2+} responses to DA and GLU in control and METH-treated astrocytes are summarized. Data represent the mean ± SEM of 54–72 cells. $^*p < 0.05$, $^{**}p < 0.01$ vs. control astrocytes.

METH (100–1000 μM) for 3 days in cortical neuron/glia co-cultures caused the robust activation of cleaved caspase-3, which is a marker of neuronal death. However, unlike METH, a high concentration of MRP failed to produce the caspase-3 activation.

In vivo astrocytic responses by METH

Finally, we investigated *in vivo* astrocytic responses in the development of METH-induced sensitization. In order to investigate the direct involvement of PKC in the development of sensitization to METH-induced hyperlocomotion, mice were given intermittently METH (2 mg/kg, s.c..) in combination with a specific PKC inhibitor NPC-15437 (1 mg/kg, s.c.). As shown in Fig. 8a, intermittent co-administration of NPC-15437 abolished the development of sensitization to METH-induced hyperlocomotion.

We also confirmed that repeated *in vivo* treatment with METH under the present schedule failed to cause the neuronal cell death; the present schedule of treatment with METH had no effect on the caspase-3 activity in the caudate putamen (data not shown).

Immunohistochemical studies were also performed in order to investigate the change in GFAP-IR levels in the cingulate cortex and nucleus accumbens following intermittent treatment with METH. As shown in Fig. 8, the GFAP-IR level was clearly increased in METH-sensitized mice compared to those in mice that had been repeatedly treated with saline. This increase in GFAP-IR level in METH-sensitized mice was completely abolished by intermittent coadministration of NPC-15437.

Discussion

Recently, astrocytes have been reported to induce synapse formation and/or stabilize CNS synapses (Barres and Smith 2001) and may be capable of integrating neuronal inputs and modulating synaptic activity. The morphological changes that occur in astrocytes produce what are collectively known as reactive astrocytes that are characterized by specific changes such as the accumulation of intermediate-filament GFAP and hyperplasia (Ridet *et al.* 1997). In the present study, we observed morphological changes in astrocytes by treatment with either METH or MRP in cortical neuron/glia co-cultures. On the other hand, a difference was noted between the effects of METH and MRP in purified cortical astrocytes: while METH markedly activated astrocytes with phosphorylation of PKC, MRP had no such effect.

In the present study, we found for the first time that treatment with METH (10 μM) for 3 days increased the sensitivity of cortical astrocytes to dopamine and glutamate; this can be responsible for rewarding effects of psychostimulants and opioids (Carlezon and Nestler 2002; Wise 2002). Many lines of evidence support the idea that the enhanced Ca^{2+} signaling in astrocytes is not restricted to single cells as Ca^{2+} can cross cell borders via gap junctions, resulting in intracellular Ca^{2+} waves traveling from one astrocyte to another, and the induction of Ca^{2+} responses in neurons (Verkhratsky and Kettenmann 1996). Taken together, these findings suggest that treatment with METH may cause the functional up-regulation of neuroactive substances in astrocytes. It is also possible that the increase in astrocytic Ca^{2+} signaling induced by dopamine and glutamate following chronic exposure to METH may result from an enhancement of astrocytic dopamine and glutamate receptor functions induced by METH.

A study of cultures of newborn rodent CNS cells has shown that heterogeneous subpopulations of astrocytes can express one or more type of opioid receptor (Ridet *et al.* 1997). It has been reported that preferential μ-opioid receptor agonists can interfere with neuronal cell division (Stiene-Martin *et al.* 2001). In the present study, we found that the μ-opioid receptor agonist MRP had no effect on astrocytic activation in cortical purified astrocytes, whereas it caused astrocytic activation in cortical neuron/glia co-cultures. These findings constitute evidence that MRP might activate

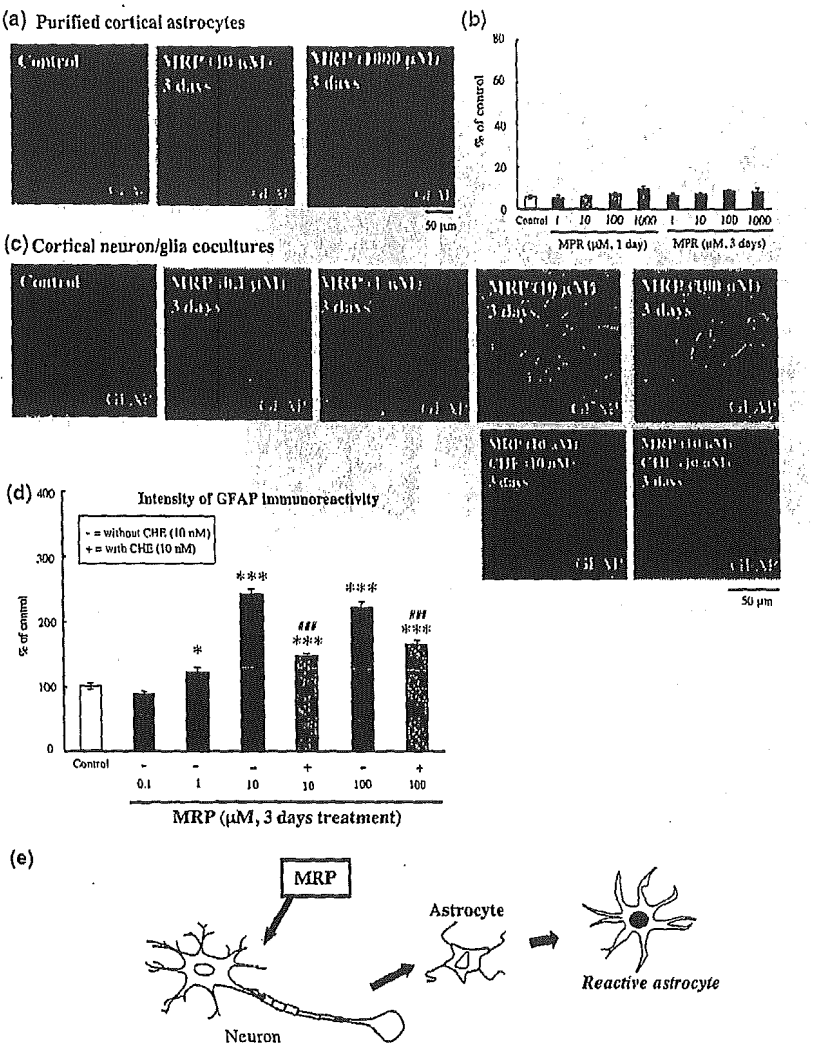

Fig. 4 Morphine (MRP) causes astrocytic activation in cortical neuron/glia co-cultures, but not in cortical purified astrocytes. (a) Purified cortical astrocytes were incubated with normal medium or MRP (10–1000 μM) for 3 days. The cells were stained with a rabbit polyclonal antibody to GFAP. (b) Purified cortical astrocytes are incubated with normal medium and MRP (1–1000 μM) for 1–3 days. Astrocytic activation as shown by a stellate morphology with processes longer than their perinuclear diameters was evaluated. Data represent the mean ± SEM of 175–230 cells from four separate observations. (c) Cortical neuron/glia co-cultures were incubated with normal medium, MRP (0.1–100 μM) or MRP (10–100 μM) + CHE (10 nM) for 3 days. The cells were stained with a rabbit polyclonal antibody to GFAP. (d) The density of GFAP-like immunoreactivity of each image was measured using NIH IMAGE. The level of GFAP like immunoreactivity on MRP- and MRP + CHE-treated cells is expressed as a percent increase (mean ± SEM) with respect to that on control cells. $^{*}p < 0.05$, $^{***}p < 0.001$; vs. control cells. $\#\#\#p < 0.001$; vs. MRP-treated cells. (e) Proposed scheme showing the mechanism of MRP-induced atrocytic activation in mouse cortical neuron/glia co-cultures.

astrocytes via neurons. Furthermore, the present results raise the possibility that METH and MRP may differentially regulate long-term changes in neuron–glia communication.

Here we demonstrated that the astrocytic activation in cortical neuron/glia co-cultures induced by either METH or MRP was blocked by treatment with a specific PKC inhibitor. PKC is a key regulatory enzyme that modulates both presynaptic and postsynaptic neuronal function, the synthesis and release of neurotransmitters, and the regulation of receptors (Narita *et al.* 2001). Several lines of evidence have suggested that *in vitro* neurite outgrowth on several cell adhesion and matrix molecules (Walsh and Doherty 1996; Powell *et al.* 2001), including fibronectin (Kuhn *et al.* 1995), laminin and collagen (Bixby and Jhabvala 1992), are reduced by the specific inhibition of PKC, suggesting that PKC plays an important role in regulating the direction of neurite growth. In our preliminary study, we found that direct PKC activation by phorbol 12,13-dibutyrate induced a robust astrocytic activation in purified cortical astrocytes (data not shown). These findings, along with those in the present study, suggest that PKC is probably one of the most important factors in modulating the synaptic plasticity induced by METH and MRP.

We also found the difference between METH and MRP in the maintenance of astrocytic activation; METH produced prolonged astrocytic activation, whereas MRP caused a reversible activation of astrocytes in cortical neuron/glia co-cultures. Astrocytic activation has been considered for a long time as the major impediment to axonal regrowth after an injury in the CNS (Ridet *et al.* 1997). However, there is increasing evidence that astrocytes play a dynamic role in regulating synaptic strength, synaptogenesis and neurogenesis (Hama *et al.* 2004). Although the exact function of METH- and MRP-induced astrocytic activation remains

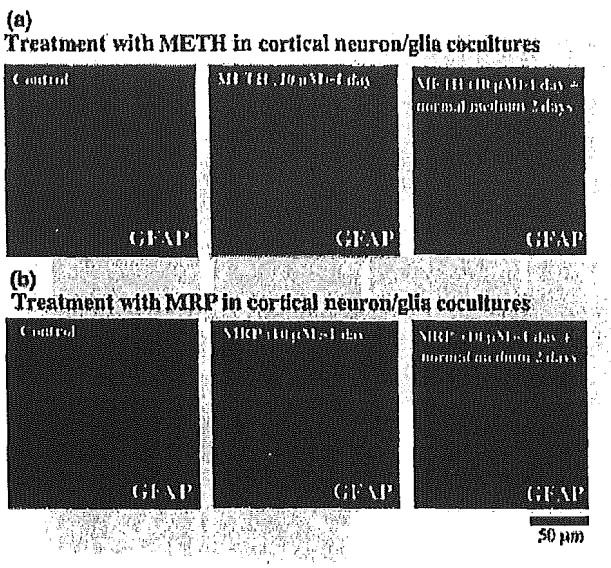

Fig. 5 METH, but not MRP, causes a long-lasting astrocytic activation in cortical neuron/glia co-cultures. (a) Cortical neuron/glia co-cultures were incubated with normal medium or METH (10 μM) for 1 day or 3 days, and cells were cultured with normal medium for additional 2 days. (b) Cortical neuron/glia co-cultures were incubated with MRP (10 μM) for 1 day or 3 day, and then, cells were cultured with normal medium for additional 2 days. All cells were stained with a rabbit polyclonal antibody to GFAP.

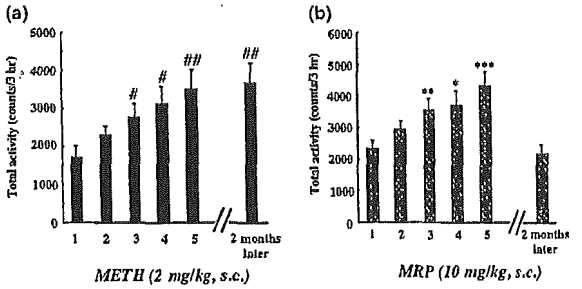

Fig. 6 The difference between METH and MRP in the maintenance of behavioral sensitization in mice. (a) Mice were treated with METH (2 mg/kg, s.c.) every 96 h for five sessions. Mice were then administered with METH (2 mg/kg, s.c.) after 2 months withdrawal. Total activity was counted for 3 h after each treatment (1, 5, 9, 13, 17 days and after 2 months withdrawal). #$p < 0.05$, ##$p < 0.01$, vs. the 1st administration. (b) Another group of mice were given five intermittent treatments morphine (10 mg/kg, s.c.) every 96 h. Mice were then administered with morphine (10 mg/kg, s.c.) after 2 months withdrawal. Total activity was counted for 3 h after the treatment (1, 5, 9, 13, 17 days and after 2 months withdrawal). *$p < 0.05$, **$p < 0.01$, ***$p < 0.001$ vs. the 1st administration.

unclear at this time, it may positively modulate synaptic activity by directly controlling synaptic strength, leading to synaptic plasticity in the CNS.

Although cultured cells used in the present *in vitro* study represents a simplication relative to the state of neuronal–glial communication in the CNS, additional interactions with these cells and matrix components in *in vivo* system are likely to reflect the behavioral change such as behavioral sensitization. In fact, one of the most important aspects of the present study was that the METH-induced behavioral sensitization was maintained even after a long period of abstinence, while the MRP-induced sensitization was reversible. This may be consistent with the evidence that METH, but not MRP, produced long-lasting astrocytic activation in cortical neuron/glia co-cultures. It is therefore worthwhile in future studies to identify the precise molecular steps associated with astrocyte–neuron signaling on a long-lasting maintenance of METH-induced behavioral sensitization.

Another key finding of the present study was that the levels of GFAP in the mouse cingulate cortex and nucleus accumbens were clearly increased by repeated *in vivo* administration of METH; this was related to behavioral sensitization (Fig. 8). These results suggest the repeated *in vivo* treatment of METH could produce the astrocytic activation in the cingulated cortex and nucleus accumbens. Central dopamine systems have been implicated in mediating reward-related behaviors. In particular, the nucleus accumbens of the mesolimbic dopamine pathway plays an important role in regulating the rewarding effects of many stimuli including drugs of abuse (Wise and Hoffman 1992). It has been also recognized that the cingulate cortex is responsible for stimulus-reward learning (Allman *et al.* 2001). Taken together, these studies suggest the possibility that METH-induced atrocytic activation in these areas modulates the development of METH-induced behavioral sensitization.

Furthermore, the development of behavioral sensitization to METH with astrocytic activation was abolished by cotreatment with the PKC inhibitor, NPC-15437. Although further experimentation is still required, these findings indicate that activated PKC-dependent astrocytic response in the cingulate cortex and nucleus accumbens by intermittent METH treatment may be implicated in the development of sensitization to the METH-induced hyper-locomotion.

Finally, we investigated the neurotoxic effects of METH and MRP; METH markedly induced neuronal cell death in cortical neuron/glia co-cultures, while MRP had no such effect. Glial activation is thought to be neuroprotective (Ridet *et al.* 1997), however, excess activation can be deleterious in the brain (Ahlemeyer *et al.* 2002). In fact, overexpression of astrocyte-derived neurotrophic protein S100β has been shown to induce neuronal cell death through nitric oxide released from astrocytes (Hu *et al.* 1997). Taken together, the present findings support the idea that the direct effect induced by high concentration of METH on astrocytes may lead to a dynamic change in neuron–glia network, resulting in the neurotoxicity.